Janne Halme, Jaakko Saarinen, and Peter Lund. 2006. Spray deposition and compression of TiO_2 nanoparticle films for dye-sensitized solar cells on plastic substrates. Solar Energy Materials & Solar Cells, volume 90, numbers 7-8, pages 887-899.

Available online at www.sciencedirect.com
SCIENCE DIRECT®
Solar Energy Materials & Solar Cells
ELSEVIER
Solar Energy Materials & Solar Cells 90 (2006) 887–899
www.elsevier.com/locate/solmat

Spray deposition and compression of TiO_2 nanoparticle films for dye-sensitized solar cells on plastic substrates

Janne Halme*, Jaakko Saarinen[1], Peter Lund

Laboratory of Advanced Energy Systems, Department of Engineering Physics and Mathematics, Helsinki University of Technology, PO Box 2200, FIN-02015 TKK, Finland

Received 10 February 2005; accepted 9 May 2005
Available online 1 July 2005

Abstract

Spray deposition of powder suspensions followed by room temperature compression was studied as a method for preparing nanostructured TiO_2 films for dye-sensitized solar cells. The structure of the films was analyzed with optical and scanning electron microscopy and the films were applied to dye-sensitized solar cells. Continuous and fast deposition of crack-free 7–14 μm thick films was achieved by heating the substrates during the deposition. Scanning electron microscopy revealed small amount of structural imperfections in the compressed films due to the nature of the deposition method. An energy conversion efficiency of 2.8% was achieved at 100 mW/cm^2 light intensity.

Keywords: Dye-sensitized; Solar cells; Nanostructured; Spray deposition; Compression

*Corresponding author. Tel.: +358 9 4513213; fax: +358 9 4513195.
E-mail address: janne.halme@tkk.fi (J. Halme).
[1]Present address. VTT Processes, Energy Production, Fuel Cells, Biologinkuja 3–5, P.O. Box 1601 FIN-02044 VTT, Finland.

0927-0248/$ - see front matter © 2005 Elsevier B.V. All rights reserved.
doi:10.1016/j.solmat.2005.05.013

1. Introduction

A dye-sensitized solar cell (DSSC) is an electrochemical device based on light absorption by sensitizer dye molecules adsorbed as a monolayer on the surface of a wide band gap semiconductor oxide nanoparticles, usually TiO_2, that form a mesoporous nanocrystalline film permeated with redox electrolyte [1,2]. The DSSC has attracted considerable interest during the past decade due to low estimated manufacturing costs combined with reasonably high energy conversion efficiencies reaching 11% at the laboratory scale [3].

Transparent conducting oxide (TCO) coated glass has been the standard choice for the substrate material of the DSSC, due to its excellent optical, electrical and encapsulation barrier properties, and compatibility with high-temperature processing. However, considerable benefits from application point of view of could be achieved if the DSSCs could be manufactured on lightweight flexible substrates such as plastic or metal foils. Flexible substrates are also a prerequisite for roll-to-roll production techniques that are considered promising for cost-effective mass production of thin film solar cells [4].

The TiO_2 photoelectrode films are usually prepared by depositing a suspension or paste containing TiO_2 nanoparticles of desired size onto a TCO coated glass or polymer substrate. The deposited film is then subject to a post-treatment with the purpose of forming a continuous nanoparticle network with sufficient adherence and electrical contact to the substrate and between the nanoparticles. Organic binders, surfactants and porosity controlling agents, which evaporate or burn off when the TiO_2 film is sintered at about 450 °C, are often used in the paste to optimize the quality of the resulting nanostructuted film. The use of plastic substrates restricts the choice of the TiO_2 suspension media and additives to those volatile at temperatures below the upper limit of the substrate material, which is about 150 °C for the commonly used polyethyleneterephtalate (PET). A mixture of TiO_2 nanoparticles and ethanol [5–8] or water [9–12] has often been used, enabling the post-treatment of the film at room temperature. Methods used for the TiO_2 film depositing include spin coating [9,13], doctor blading [5–8,10,11,14–18], electrophoretical deposition [19–22] and spraying [23].

Among a variety of methods used for the low-temperature post-treatment of the nanostructured TiO_2 films, including low-temperature sintering [9–11,13,14,18,23], hydrothermal crystallization [15–17], chemical vapor deposition of Ti alkoxides [19–21], microwave irradiation [21,24], UV light irradiation [18–20], electron bombardment [25], and interparticle binding by a TiO_2 nanoparticle sol [22], the room temperature compressing technique [5–8,12,26] is particularly promising for roll-to-roll production because it can be performed rapidly and in a continuous manner using calendering techniques well known from paper technology. Efficiencies of 2.3% [5] and 2.5% [8] at the standard conditions of 100 mW/cm^2 light intensity with AM1.5 spectrum have been reported for solar cells with the TiO_2 electrodes prepared on ITO-PET substrates by the compressing technique. Similar or higher efficiencies (2.3–4.3%) have been reported for other deposition and post-treatment methods [16,17,19–22,27].

The objective of this work was to investigate the applicability of spray deposition combined with room temperature compressing to the preparation of nanostructured TiO_2 films on plastic substrates for DSSCs. The structural quality of the resulting TiO_2 films was investigated by optical microscopy (OM) and scanning electron microscopy (SEM). The films were applied as photoelectrodes in DSSCs, and the performance of the solar cells was characterized by current—voltage (I–V) measurements in a solar simulator.

The results demonstrate that spray deposition of TiO_2 films from nanoparticle suspensions can be successfully combined with compression at room temperature. The method produces a good quality photoelectrodes and gives several practical advantages over the conventional doctor blading method in the deposition of low viscosity TiO_2 suspensions.

2. Materials and methods

2.1. Preparation of the TiO_2 films

TiO_2 suspensions containing 20 wt% of nanocrystalline TiO_2 powder (P25 from Degussa) were prepared by mixing the powder with either ethanol (98%) or de-ionized water followed by stirring with a magnetic stirrer for a few hours.

Indium tin oxide (ITO) coated polyethyleneterephtalate (PET) sheets (NV-CT-CHO1S-M-7 from Bekaert Specialty Films), with 20 mm × 20 mm size, 190 μm thickness and approximately 60 Ω/square sheet resistance, were used as substrates. The substrates were cleaned in mild solution of Sigmaclean® detergent in de-ionized water in an ultrasonic bath at 50 °C for 3 min followed by rinsing with de-ionized water, acetone and ethanol, and dried in a stream of pressurized air.

The ITO-PET substrates were laid on a heating plate at 80–100 °C and the TiO_2 suspension was sprayed onto the substrate with an Aztek A320 airbrush connected to a Sparmax AC-100 air compressor. A piece of an overhead projector transparency was used as a frame to define the area and position of the TiO_2 film on the substrate. Distance between the spray nozzle and the substrate was approximately 15 cm.

The compression of the TiO_2 films was performed with an MTS 810 Material Testing System. The TiO_2 coated ITO-PET substrate was placed between two planar stainless steel plates. 50–150 μm thick Teflon® PTFE-films (from Fluorplast) served as protective sheets to prevent adhesion of the TiO_2 powder on the upper plate of the press. The compression was performed at the room temperature with 50 kN/s ramps from zero to a maximum pressing force of 3.8–9.6 kN (6–15 kN/cm^2 of the TiO_2 film area) with a 1 s holding time. It is likely that some of the compression pressure was also absorbed by the uncoated areas of the substrate but the exact pressure distribution could not be determined. Equally sized substrates were used in all samples to have repeatable pressing conditions. The applied compressing pressures are well within the range used in the roll-to-roll calendaring in paper processing, where typical nip pressures are up to several hundred kN/m.

2.2. Preparation of the solar cells

The compressed TiO_2 films were dye-sensitized by soaking the films for 20–44 h in a dye solution consisting of 0.3 mmol/dm^3 *cis*-bis(isothiocyanato)bis(2,2′-bipyridyl-4,4′-dicarboxylato)-ruthenium(II) bis-tetrabutylammonium dye (N719) from Solaronix in ethanol (98%). Before immersing into the dye solution, the films were heated to 100–120 °C on a heating plate to remove physisorbed water. The dye-sensitization took place at the room temperature in dark in a closed container without stirring of the dye solution. After the dye impregnation, the films were rinsed with ethanol and dried in air. The assembling of the solar cell followed directly after this to minimize the time of exposure of the dry dye-sensitized TiO_2 film to the ambient air.

Counter electrodes were prepared on fluorine doped tin oxide (FTO) coated glass substrates (Pilkington TEC 15 from Hartford Glass, sheet resistance 15 Ω/square) using the thermal platinum cluster catalyst method [28]. The substrates were cleaned in the same way as the ITO-PET substrates. A few droplets of platinum solution consisting of 5 mmol/dm^3 $PtCl_4$ (98%, Aldrich) in isopropanol (99.7%, Merck) was spread on the substrate and dried in the ambient air. Finally the substrates were fired in an oven at 385 °C for 15 min and then cooled to room temperature.

The solar cells were assembled by placing the dye-sensitized TiO_2 electrode and the counter electrode together in a sandwich structure using 60 μm thick Surlyn® 1702 film (DuPont) as spacer and edge sealant. Adherence of the Surlyn film to the substrates was induced by pressing the substrates together on a heating plate at 100 °C. This reduced the film thickness to about 40 μm. An electrolyte solution consisting of 0.5 mol/dm^3 LiI (99%, Merck), 50 mmol/dm^3 I_2 (99%, Prolabo), 0.5 mol/dm^3 4-*tert*-butylpyridine (99%, Aldrich) in 3-methoxypropionitrile (98%, Aldrich) was applied between the electrodes through channels left in the Surlyn sealant. The channels were sealed with TorrSeal® vacuum sealant (Varian). Current collector contacts were made from a copper tape (Chomerics) placed along one edge of each substrate. Electrolube® conductive silver paint was used to secure good electrical contact between the copper tape and the TCO layer of the substrate. Both electrodes were rectangular of 8 mm × 8 mm size and these were positioned in one corner of the 20 mm × 20 mm substrate at a 2 mm distance from the edge of the substrate. The width of the sealant rim was also 2 mm, and the distance between the edge of the electrode and the current collector was 2–3 mm.

2.3. Characterization

Optical microscopy was performed at dia-illumination with a Nikon type 104 microscope equipped with a 3CCD color video camera (JVC model KY-F55B) connected to a computer.

SEM was performed in secondary electron imaging detection mode with LEO DSN 982 Gemini field emission scanning electron microscope with 2 kV acceleration voltage. The samples for SEM analysis were prepared on FTO coated glass to improve image quality: samples on ITO-PET produced blurred micrographs at the

highest magnifications, possibly due to local heating and deformation of the plastic substrate under the electron beam.

The thickness of the TiO_2 films was measured with a micrometer within $\pm 2\,\mu m$ accuracy. The surface density of the deposited TiO_2 films was determined by measuring the mass of the substrates with Mettler M3 scales before and after film deposition and compression, and was subject to an uncertainty of $\pm 50\,\mu g/cm^2$ due uncontrolled absorption of water from the ambient air by the PET substrate.

The photovoltaic measurements were performed with a solar simulator using halogen lamps (Philips 13117) as a light source. The light intensity was adjusted to correspond to $100\,mW/cm^2$ with AM1.5G solar spectrum with a monocrystalline silicon reference solar cell (PVM 19 from PV Measurements) calibrated by NREL. Spectral mismatch correction (correction factor 1.06) was performed to the measured solar cell currents [29].

Current—voltage curves were measured with Keithley 2420 SourceMeter®, keeping the solar cells at 25 °C by Peltier elements.

3. Results and discussion

3.1. Spray deposition

Our work with the spray deposition was motivated by difficulties encountered in producing uniform, well adhered and crack-free films of about 10 μm thickness in one deposition step from TiO_2 suspensions in ethanol or water with the common doctor blading technique using a tape as a frame. Such problems have been reported previously and have been attributed to the high surface tension in the TiO_2 suspensions in the absence of organic additives [5–7,9,13]. We observed that the surface tension in the suspension tended to pull material to the edges of the tape frame and the film uniformity was sensitive to the way the glass rod was operated (speed and steadiness). Variation of the film thickness was complicated because of increased tendency of the film to cracking and flaking during drying, as the deposition thickness of the film was increased. The problem has been previously tackled by performing successive deposition—post-treatment cycles of thin layers [9,13], using a low surface tension suspension liquid such as ethanol [5–7] or adjusting the composition of the TiO_2 suspension [12].

It turned out that with the spray deposition technique uniform crack-free TiO_2 powder films with desired thickness (up to 20 μm after compression) could be easily prepared from TiO_2–ethanol suspensions. Also the thickness of the deposited TiO_2 film could be easily varied. Cracking of the film during drying was effectively prevented by performing the deposition in short pulses giving the suspension liquid enough time to evaporate in between. The evaporation rate could be enhanced by heating the substrate to 80–100 °C during spraying which allowed also continuous deposition and prevented uncontrolled spreading of the suspension on the substrate. The deposited films were adhered to the substrate well enough to sustain handling in the later stages of the preparation. Similar crack-free films were obtained also with

TiO_2—water suspensions. In this case more time was needed for the evaporation of the liquid between the spray pulses.

3.2. Optical microscopy

Fig. 1 shows optical microscopy images of the front surface and cross-section of a typical spray deposited TiO_2 film after drying but before compression. The film is highly porous consisting of spherical TiO_2 powder agglomerates with 5–30 μm diameter, randomly distributed over the substrate and in contact with each other. The inset in Fig. 1(a) reveals some inner structure in an agglomerate of 14 μm diameter suggesting that also the agglomerates themselves are highly porous. It can be easily concluded that the local TiO_2 surface density varies significantly and in a random manner over the substrate in the uncompressed film.

The agglomerated structure of the deposited film is a consequence of the droplet nature of the spray deposition each powder agglomerate originating from a single spray droplet. The porosity of the film in the micrometer scale was affected by the wetness of the film during deposition which could be controlled to some extent by the substrate temperature and deposition rate. When the deposition of the TiO_2–ethanol suspension was performed in a single long spray pulse without heating the substrate,

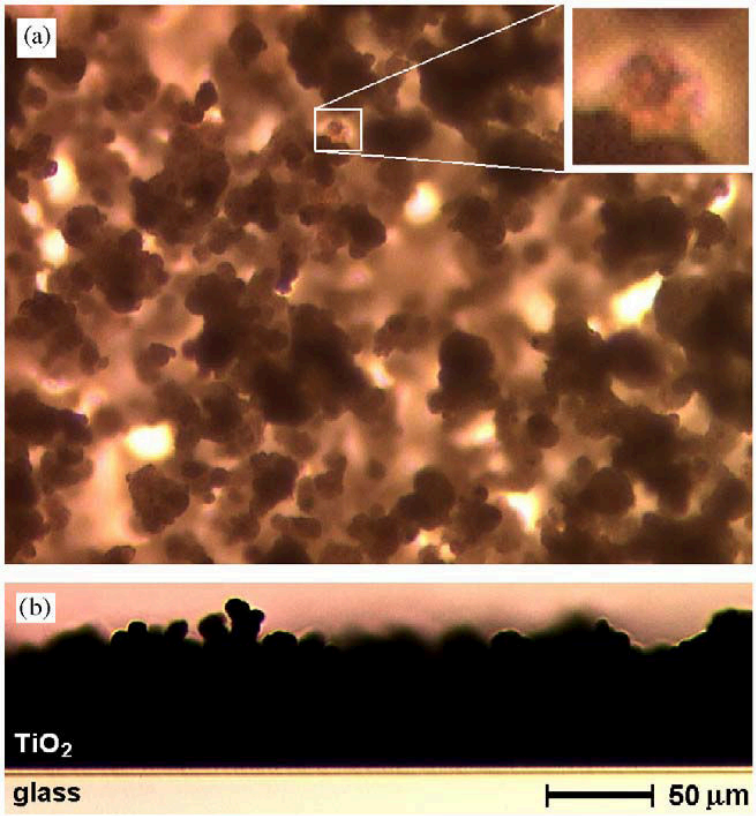

Fig. 1. Optical microscopy images of TiO_2 films spray deposited from an ethanol based particle suspension. (a) Front image. The inset shows a magnified image of a single spray particle. (b) Cross-section image. The 50 μm scale applies to both images.

the film was wet during the deposition resulting in a smooth film surface in the micrometer scale but cracking of the film during drying. When the substrate was heated to about 80–100 °C, and the deposition was performed in sufficiently small doses, a highly porous macroscopically uniform agglomerated film similar to that in Fig. 1 was obtained. Between these extremes, films with different porosity and level of agglomeration could be produced. This behavior suggests that the TiO_2 powder agglomerates form inside the spray droplets and maintain their integrity when hitting the substrate if evaporation of the suspension liquid is sufficiently fast compared to the deposition rate. The ability of this technique to produce crack-free films can be understood based on the structure of the deposited film (Fig. 1). Because the integrity of the TiO_2 powder agglomerates was preserved during drying of the film, the pores between the agglomerates grew instead of forming macroscopic cracks in the film.

3.3. Electron microscopy

Fig. 2 shows scanning electron micrographs of a spray deposited and compressed TiO_2 film on an FTO glass substrate. The cross-section image in Fig. 2a shows that the compression of the spray deposited film has produced a continuous 13.5 μm thick

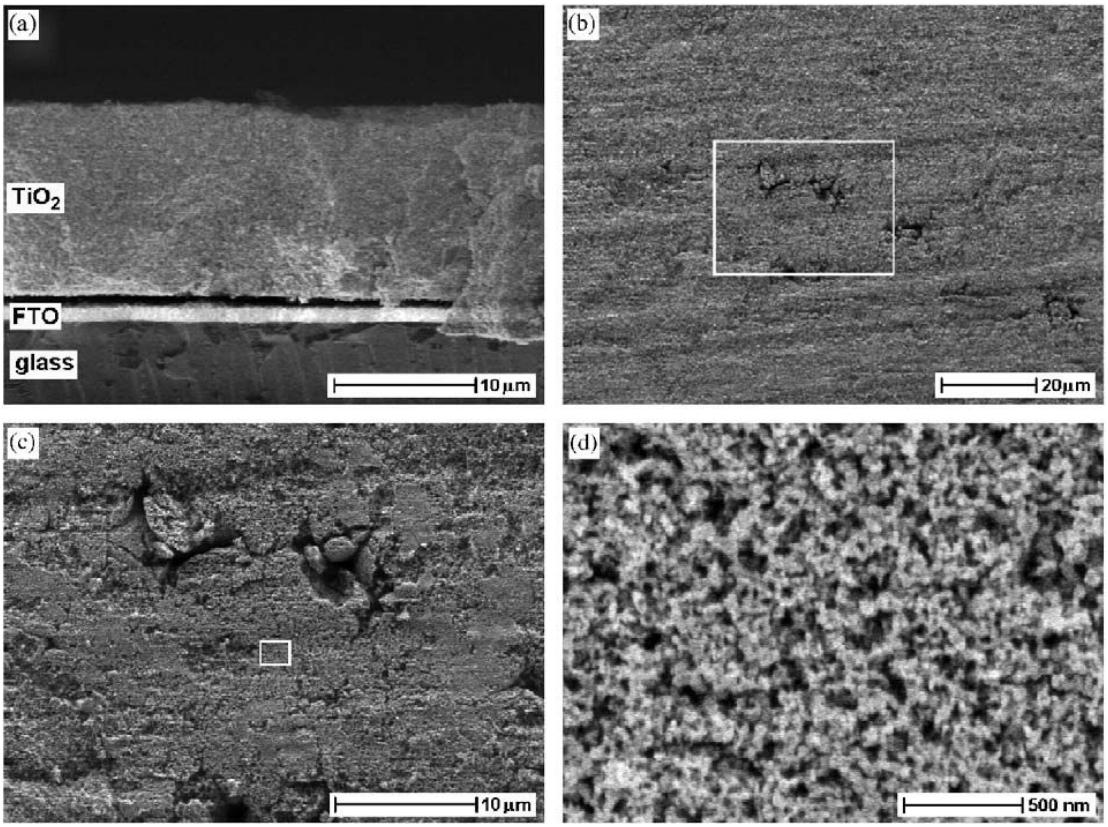

Fig. 2. Scanning electron micrographs of a TiO_2 nanoparticle film spray deposited from ethanol solution on FTO-coated glass substrate and compressed at ca. 6 kN/cm^2 pressure. (a) A cross-section image. (b)–(d) front surface images at different magnifications. The white rectangle in (b) and (c) marks the position of the magnified image in (c) and (d), respectively.

TiO_2 film. No traces of the stepwise spray deposition method in the form of individual layers can be seen. This is expected because of the very high porosity and the agglomerated nature of the uncompressed film (Fig. 1).

The gap seen between the TiO_2 film and the underlying FTO layer in Fig. 2a was caused by the sample preparation, i.e. cutting the substrate, and is not an inherent property of the film. This is supported by the fact that such gaps extended several hundred micrometers over the film edge in the SEM images (data not shown), yet the TiO_2 films were well adhered to the substrate. A thin flake of TiO_2 film hanging in front of the cross-section on the right side in Fig. 2a is another artifact from the sample preparation.

The front surface image of the TiO_2 film at low magnification in Fig. 2b shows that the film is mostly smooth and uniform in thickness along the surface on a scale of a few tens of micrometers. Comparing to Fig. 1, it can be easily concluded that the TiO_2 spray particles have collapsed during compression and the TiO_2 powder material has been redistributed over the substrate.

However, some irregular holes about 8 μm in diameter can be seen in the film (Fig. 2b–c). The inward curved edges of the holes (Fig. 2c) suggest that they have been formed as some of the largest pores between the spherical TiO_2 agglomerates in the uncompressed film have not been completely closed by the redistribution of the powder material during compression. The size of the holes also matches that of the pores in the uncompressed film (Fig. 1).

The fact that some holes remain in the film after compression indicates that the compression is not able to even out completely the random variation in the TiO_2 surface density that is characteristic to the uncompressed spray deposited film. This suggests that those areas in the film that seem uniform in thickness in the front surface SEM images in the micrometer scale (Fig. 2b–c), may however have variation in TiO_2 surface density, due to variation of porosity in the bulk part of the film. Due to the compression method applied and the high porosity of the uncompressed film, the variation of the TiO_2 surface density does not lead to variation in the thickness of the compressed film (Fig. 2b).

It has been shown that the porosity of the compressed TiO_2 nanoparticle films depends on the applied compression pressure, the porosity being lower for a higher compression pressure [6]. We may also conclude that in the regions of lower porosity the powder material may have been subject to lower effective compression pressure than in the regions of higher porosity.

Information on porosity inside the film is not readily available from the SEM surface images except for the uppermost particle layers (Fig. 2d). Areas with different surface roughness can be seen in Fig. 2c which could be partly due to variation in the surface density of TiO_2, high surface roughness indicating high local film porosity. However, a more likely reason to the variation in the surface roughness may be the TiO_2 powder material has adhered in some places to the PTFE cover sheet during the compression.

We also observe that a pattern of parallel horizontal lines in Fig. 2b has been printed on the surface of the film. Comparing Fig. 2b and c, it can be concluded that the rough area in the upper part of Fig. 2c is part of this lineation pattern suggesting

that the local surface roughness of the final TiO_2 film is affected by the compression process and the surface texture of the PTFE cover sheet. The local surface morphology of the film can therefore not be reliably related to the porosity of the underlying bulk film. The surface texture of the PTFE cover sheets may induce further variation in the local compression pressure.

Some variation in the surface density of TiO_2, porosity of the film, and effective compression pressure is expected due to the random nature of the spray deposition. However, redistribution of the powder material is the more effective, the larger the thickness of the deposited film. The film uniformity could be improved by reducing the spray droplet size, which increases the number of the powder agglomerates per surface area of the substrate. The size of the spray droplets was not known directly, but if we assume that the porosity of the TiO_2 powder agglomerates in the uncompressed film (Fig. 1) is 80%, a typical 20 μm agglomerate diameter would correspond to a 38 μm droplet diameter for a 20 wt % TiO_2–ethanol solution, assuming that the P25 TiO_2 powder is 30% anatase and 70% rutile by mass [6].

Fig. 2d shows a magnification of a relatively smooth and hole-free part of the film. The mesoscopic structure of the film is close to that of a compressed film deposited by doctor blading from the same TiO_2 material and solution [6]. The TiO_2 particles are randomly distributed over the film surface. The primary particle size of the Degussa P25 TiO_2 powder determined from a SEM image at $\times 200\,000$ magnification (data not shown) ranged between 20–60 nm which is in consistence with results of other studies, e.g. [26].

Although the sample for the SEM analysis was prepared on glass, these conclusions should be valid for corresponding TiO_2 films prepared on ITO-PET substrates. No signs of deformation of the ITO-PET foil due to compressing the TiO_2 film were found by visual inspection and optical microscopy. Separate experiments confirmed that the compression did not induce any changes to the conductivity of the ITO layer underneath the TiO_2 film or across the edge of the film.

3.4. Solar cell performance

Fig. 3 shows current–voltage curves of solar cells prepared from the spray deposited and compressed TiO_2 films using either ethanol (series A) or water (series B) in the powder suspension. The corresponding characteristic I–V parameters and relevant information of the TiO_2 films are shown in Table 1.

The TiO_2 films deposited from the ethanol based particle suspension showed a higher short-circuit current density, open-circuit voltage and conversion efficiency than films deposited from the water based suspension. Because the cell series A and B were prepared from different batches of electrolyte and dye solutions, effects due to differences in the preparation conditions between the series cannot be fully ruled out.

The short-circuit current density and the conversion efficiency exhibit rather large standard deviations within the cell series indicating low reproducibility in the cell preparation at this stage. Relatively large standard deviation in the conversion efficiencies seems to be typical to series of DSSCs prepared manually over a long time period [7,12]. Mainly due to the weak reproducibility along with uncertainties in

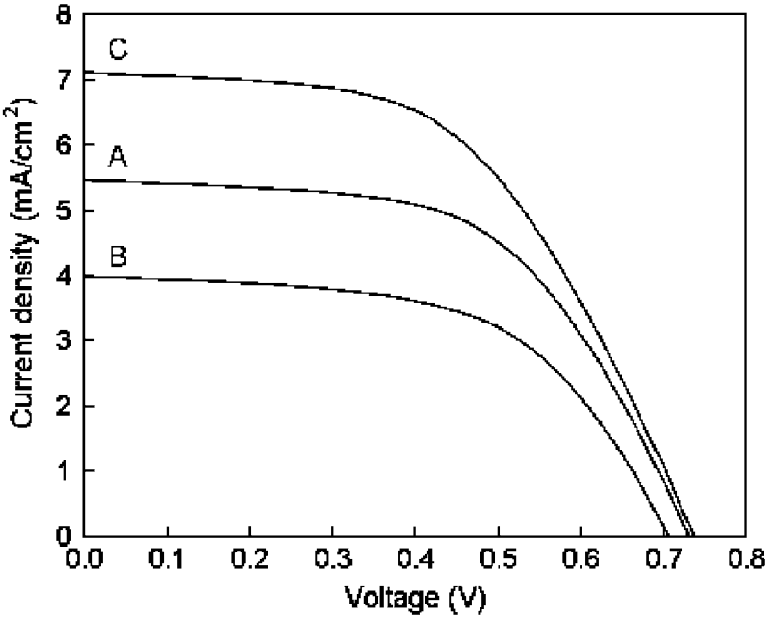

Fig. 3. Average I–V curves of the solar cell series A, B and C. Measurements were performed at 100 mW/cm^2 AM.15G equivalent illumination.

film thickness and mass measurements, no strong relation between the solar cell performance and the TiO_2 film thickness was found in the surface density range 1000–1900 μg/cm^2.

The room temperature compressed TiO_2 photoelectrodes spray deposited from an ethanol based particle suspension gave solar cell efficiencies ($2.3 \pm 0.2\%$, Table 1) that are in the same range as those obtained by others with compressed TiO_2 films on ITO-PET substrates deposited by the doctor blading method (2.3% [5], $2.5 \pm 0.2\%$ [8], measured at 100 mW/cm^2 AM1.5 light intensity). The efficiency of the solar cell C (Table 1), representing the best cell performance (2.8%) achieved in this work on ITO-PET is slightly higher than these previous results.

Compared to the highest efficiencies reported for plastic DSSCs by other TiO_2 deposition and post-treatment methods (4.3% [27]), or to the record efficiencies on FTO-glass substrates (ca. 11% [3]), at the 100 mW/cm^2 AM1.5G conditions, the results of the present study remain more modest. A reason to this is the voltage losses due to the resistance in the TCO layers of the substrates, especially since the geometry of the cells in this study was not optimized in respect to this factor. According to our measurements with electrochemical impedance spectroscopy, the charge transfer resistance at the Pt counter electrodes in the present case is typically 4–5 Ω cm^2, causing only minimal drop in the fill factor. Furthermore, the ion transport is expected not to limit the current density, nor cause significant concentration overpotentials at the counter electrode. The relatively low short-circuit current densities, irrespective of the TiO_2 film thickness, are most likely due to insufficient collection efficiency of photoelectrons from the compressed TiO_2 film [12].

Table 1
Average performance results of solar cells prepared by spray-deposition and compression of nanostructured TiO_2 films on ITO-PET substrates

	No. of samples	TiO_2 solvent	Compression pressure (kN/cm^2)	Surface density ($\mu g/cm^2$)	Thickness (μm)	V_{OC} (V)	I_{SC} (mA/cm^2)	*FF*	η (%)
A	4	Ethanol	10	1000–1400	7–10	0.73 ± 0.01	5.5 ± 0.5	0.57 ± 0.02	2.3 ± 0.2
B	8	H_2O	10	1300–1900	10–14	0.71 ± 0.01	4.0 ± 0.6	0.58 ± 0.05	1.6 ± 0.3
C	1	Ethanol	15	1500	11	0.74	7.1	0.53	2.8

Measurements were performed at $100\,mW/cm^2$ AM1.5G equivalent illumination.
V_{OC} is the open-circuit voltage; I_{SC} the short-circuit current density; *FF* the fill factor; η the energy conversion efficiency.

Considering the structural unevenness of the TiO_2 films in the microscopic scale (Fig. 2), these initial results from the spray deposition are promising and leave room for further optimization of the method.

4. Conclusions

The spray deposition of TiO_2 nanoparticle suspensions on heated substrates was found to be a fast and effective method for preparing crack-free TiO_2 powder films of desired thickness for the subsequent post-treatment by compression at the room temperature without any organic additives in the TiO_2 suspension. A relatively good solar cell performance of 2.8% at 100 mW/cm^2 light intensity was achieved with the method.

The critical point in the described spray deposition method is the successful control of the evaporation rate of the suspension liquid with respect to the deposition rate. This preserves the agglomerated nature of the deposited film originating from the spray droplets and prevents macroscopic cracking and flaking of the film during drying. The highly porous and agglomerated structure of the deposited films is compatible with the compression as the post-treatment step. The obtained solar cell performances and the SEM analysis indicate that it is not necessary to have a compact structure in the deposited nanoparticle film prior to the compression step. The drawback of the spray deposition is, however, the variation in the local surface density of deposited material which results in structural unevenness in the compressed film. The TiO_2 film quality could be improved by optimizing the spray droplet size and the TiO_2 concentration of the powder suspension. Based on our observations, there likely exist optimum deposition conditions wet enough to give microscopically homogenous film quality but still adequately dry to prevent cracking and flaking of the film. The results presented here correspond to the dry end of the deposition conditions.

The spray deposition was successful also with the water based TiO_2 suspensions indicating that the surface tension of the suspension liquid is not a crucial parameter in the spray deposition. The spray deposition method may therefore offer larger flexibility in selecting the suspension liquid than the doctor blading technique. Finally, the successful control of the TiO_2 film quality and the increased deposition rate achieved by heating the substrate makes the spray deposition method promising from the point of view of roll-to-roll production of nanostructured TiO_2 films for flexible dye-sensitized solar cells.

Acknowledgments

Financial support from the National Technology Agency of Finland (Tekes) is gratefully acknowledged. J. H. is grateful for the scholarship from the Nordic Energy Research (NEFP). The authors thank Dr. Jani Kallioinen for providing the ITO-PET substrates, Degussa for supplying the P25 powder and DuPont for supplying

the Surlyn® sheets. The authors also thank Dr. Jouni Paltakari and Mr. Harri Jaronen for carrying out the compression of the TiO_2 films, and Dr. Unto Tapper for the SEM imaging.

References

[1] B. O'Regan, M. Grätzel, Nature 353 (1991) 737–740.
[2] M.K. Nazeeruddin, A. Kay, I. Rodicio, R. Humphry-Baker, E. Müller, P. Liska, N. Vlachopoulos, M. Grätzel, J. Am. Chem. Soc. 115 (1993) 6382–6390.
[3] M. Grätzel, J. Photochem. Photobiol. A 164 (2004) 3–14.
[4] A. Shah, P. Torres, R. Tscharner, N. Wyrsch, H. Keppner, Science 285 (1999) 692–698.
[5] H. Lindström, A. Holmberg, E. Magnusson, S. Lindquist, L. Malmqvist, A. Hagfeldt, Nano Lett. 1 (2001) 97–100.
[6] H. Lindström, E. Magnusson, A. Holmberg, S. Södergren, S. Lindquist, A. Hagfeldt, Solar Energy Mater. Solar Cells 73 (2002) 91–101.
[7] H. Lindström, A. Holmberg, E. Magnusson, L. Malmqvist, A. Hagfeldt, J. Photochem. Photobiol. A 145 (2001) 107–112.
[8] S.A. Haque, E. Palomares, H.M. Upadhyaya, L. Otley, R.J. Potter, A.B. Holmes, J.R. Durrant, Chem. Commun. 24 (2003) 3008–3009.
[9] S. Ito, T. Takeuchi, T. Katayama, M. Sugiyama, M. Matsuda, T. Kitamura, Y. Wada, S. Yanagida, Chem. Mater. 15 (2003) 2824–2828.
[10] S. Nakade, M. Matsuda, S. Kambe, Y. Saito, T. Kitamura, T. Sakata, Y. Wada, H. Mori, S. Yanagida, J. Phys. Chem. B 106 (2002) 10004–10010.
[11] M. De Paoli, A.F. Nogueira, D.A. Machado, C. Longo, Electrochim. Acta 46 (2001) 4243–4249.
[12] A. Hagfeldt, G. Boschloo, H. Lindström, E. Figgemeier, A. Holmberg, V. Aranyos, E. Magnusson, L. Malmqvist, Coord. Chem. Rev. 248 (2004) 1501–1509.
[13] F. Pichot, J.R. Pitts, B.A. Gregg, Langmuir 16 (2000) 5626–5630.
[14] P.M. Sommeling, M. Späth, J. Kroon, R. Kinderman, J. van Roosmalen, European photovoltaic solar energy conference, Proceedings of the International Conference, 16th, Glasgow, United Kingdom, May 1–5, 2000, vol. 1, 2000, pp. 67–71.
[15] D. Zhang, T. Yoshida, H. Minoura, Chem. Lett. (2002) 874–875.
[16] D. Zhang, T. Yoshida, H. Minoura, Adv. Mater. 15 (2003) 814–817.
[17] D. Zhang, T. Yoshida, K. Furuta, H. Minoura, J. Photochem. Photobiol. A 164 (2004) 159–166.
[18] C. Longo, J. Freitas, M. De Paoli, J. Photochem. Photobiol. A 159 (2003) 33–39.
[19] T.N. Murakami, Y. Kijitori, N. Kawashima, T. Miyasaka, Chem. Lett. 32 (2003) 1076–1077.
[20] T.N. Murakami, Y. Kijitori, N. Kawashima, T. Miyasaka, J. Photochem. Photobiol. A 164 (2004) 187–191.
[21] T. Miyasaka, Y. Kijitori, T.N. Murakami, M. Kimura, S. Uegusa, Chem. Lett. (2002) 1250–1251.
[22] T. Miyasaka, Y. Kijitori, J. Electrochem. Soc. 151 (2004) A1767–A1773.
[23] K.C. Mandal, A. Smirnov, D. Peramunage, R.D. Rauh, Mater. Res. Soc. Symp. Proc. 737 (2003) 739–744.
[24] S. Uchida, M. Tomiha, H. Takizawa, M. Kawaraya, J. Photochem. Photobiol. A 164 (2004) 93–96.
[25] T. Kado, M. Yamaguchi, Y. Yamada, S. Hayase, Chem. Lett. 32 (2003) 1056–1057.
[26] P. De Almeida, J. van Deelen, C. Catry, H. Sneyers, T. Pataki, R. Andriessen, C. van Roost, J.M. Kroon, Appl. Phys. A (2003).
[27] R. Kumar, A.K. Sharma, V.S. Parmar, A.C. Watterson, K.G. Chittibabu, J. Kumar, L.A. Samuelson, Chem. Mater. 16 (2004) 4841–4846.
[28] N. Papageorgiou, W.F. Maier, M. Grätzel, J. Electrochem. Soc. 144 (1997) 876–884.
[29] C.H. Seaman, Solar Energy 29 (1982) 291–298.